

# The $m/n=1/1$ Instabilities in An EAST NBI Discharge\*

Qing-Yun Hu(胡庆云)<sup>1</sup>, Li-Qing Xu(徐立清)<sup>2</sup> and Dong-Jian Liu(刘东剑)<sup>1\*\*</sup>

<sup>1</sup>College of Physics, Sichuan University, Chengdu 610065, China

<sup>2</sup>Institute of Plasma Physics, Chinese Academy of Sciences, Hefei 230031, China

An analysis of precession fishbone, diamagnetic fishbone and internal kink mode in Tokamak plasmas are presented via solving the fishbone dispersion relation. Applying the dispersion relation to EAST discharge experiment, excitation of precession fishbone due to Neutral Beam Injection is successfully explained. Real frequency and growth rate of diamagnetic fishbone and internal kink mode are calculated.

**PACS:** 52.30.Cv, 52.30.Ex, 52.30.Gz, 52.35.-g, 52.35.Py, 52.55.Tn

---

## 1. Introduction

Fishbone instabilities, excited by energetic particles (EPs) in magnetic confined plasmas often result in loss of energetic particles, degrading confinement of plasmas and the heating efficiency. Since the first observation of fishbones in Poloidal Divertor Experiment (PDX) tokamak in 1983 [1], two kinds of models have been proposed to explain the excitation of fishbone instabilities. The first model, given by *Chen et al* indicates that EPs have a destabilizing effect on internal kink modes. One outcoming mode, which has a real frequency comparable to the trapped particles' toroidal precession frequency, is referred to as the precession fishbone [2] [3]. The other model, taking Finite ion Larmor radius (FLR) effects into account, was first suggested by *Coppi et al* [4] [5]. Ideal MHD instability was rendered marginally stable by FLR, creating a new MHD mode which mode-particle resonance was needed to grow. Since this mode has a real frequency related to ion diamagnetic frequency, it is referred to as diamagnetic fishbone. There is another solution in this model which is considered to origin from the internal kink mode, with a frequency even lower.

Fishbone oscillations have been observed in EAST Neutral-Beam-Injection (NBI) experiments [6]. This branch of fishbone, with a frequency at the same order of precession frequency of trapped EPs, is the product of interaction between Energetic Particle Modes (EPM) and Internal Kink Modes. The coupling behavior between EPs and Internal Kink modes not only brings change to  $m/n=1/1$  internal kink mode but also drives fishbone modes. Fishbone modes are often accompanied by sawtooth crash in EAST, but the mechanism between the two phenomena remains unclear. Because of the destructive effect sawtooth have on confinements, it is an urge to have an investigation on fishbones in EAST discharges thoroughly.

In this paper, adopting real experiment data from an EAST NBI discharge and using the combined dispersion relation from both fishbone models, we studied the fishbone instabilities.

Three branches of modes are shown in numerical calculations. The behavior of real frequencies and growth rates are calculated as  $\beta_h$  changes. Base on analytical and numerical calculations, we find the criteria  $\beta_{h,c}$  without ion diamagnetic effect and the modified  $\beta_{h,c}$  as FLR is considered, showing the influence of pressure gradient on precession fishbone. Then we have a discussion on the diamagnetic branch and the internal kink.

## 2. Dispersion relation

In this work, under the assumption of large aspect ratio circular cross-section plasma equilibrium, deeply trapped energetic ions are treated with drift kinetic equations while background plasmas are described in resistive MHD closure. With the generalized energy principle, the dispersion relation of fishbone modes can be written as

$$\delta\hat{I} + \delta\hat{W}_c + \delta\hat{W}_k = 0 \quad (1)$$

The first term  $\delta\hat{I}$  is a normalized inertia of inner layer;  $\delta\hat{W}_c$  stands for a normalized ideal MHD potential energy variation of background plasmas; The nonadiabatic kinetic contributions from EPs is represented by  $\delta\hat{W}_k$ .

In the case where finite ion gyro-radius and drift wave frequency effects are retained,  $\delta\hat{I}$  reads [7]

$$\delta\hat{I} = -\frac{8i\Gamma[(\Lambda^{3/2} + 5)/4]}{\Lambda^{4/3}\Gamma[(\Lambda^{3/2} - 1)/4]} \frac{[\omega(\omega - \omega_{*i})]^{1/2}}{\omega_{A\theta}} \quad (2)$$

Where  $\Lambda = \frac{-i[\omega(\omega - \omega_{*i})(\omega - \hat{\omega}_{*e})]^{1/3}}{S_M^{-1/3}\omega_{A\theta}}$ ;  $S_M$  denotes the Reynolds number,  $S_M = \tau_R/\tau_A$ ,  $\tau_R = \mu_0 r_s^2/\eta$ ,  $\tau_A = \omega_{A\theta}^{-1}$ ;  $\omega_{A\theta}$  is the shear Alfvén frequency,  $\omega_{A\theta} = \frac{B_\theta s}{r_s \sqrt{4\pi\rho}}$ , and  $B_\theta, s, \rho$  are poloidal magnetic field, magnetic shear, mass density, respectively;  $\omega_{*i}$  is ion diamagnetic frequency;  $\hat{\omega}_{*e} = \omega_{*e} + 0.71 \frac{c}{eBr_s} (\frac{dT_e}{dr})_\eta$  with  $\omega_{*e}$  the electron drift wave frequency.

For a parabolic  $q$  profile,  $\delta\hat{W}_c$  is calculated to be [8]  $3\pi \left(\frac{r_s}{R_0}\right)^2 (1 - q_0)(13/144 - \beta_p^2)$  with  $\beta_p = -\frac{2\mu_0}{B_\theta^2(r_s)} \int_0^1 dx x^2 dP/dx$ .  $R_0$  is the main radius;  $q_0$  is the safety factor at magnetic axis;  $x = r/r_s$ .

For deeply trapped energetic ions with a slowing-down distribution  $F_{h0} = n(r)\delta(\alpha - \alpha_0)E^{-3/2}$ , the nonadiabatic kinetic contribution is expressed as [9]

$$\delta\hat{W}_k = \beta_h \frac{1}{\varepsilon} \frac{\omega}{\omega_{dm}} \ln \left( 1 - \frac{\omega_{dm}}{\omega} \right) \quad (3)$$

With  $\beta_h$  denoting the spatial average of trapped particle  $\beta$  within  $q=1$  surface;  $\omega_{dm}$  denoting precessional drift frequency evaluated at a characteristic energy  $E_m$ ;  $\varepsilon$  is a parameter related to the density gradient.

Now we can write the dispersion relation as follows:

$$-\frac{8i\Gamma[(\Lambda^{3/2} + 5)/4]}{\Lambda^4\Gamma[(\Lambda^{3/2} - 1)/4]} \frac{[\omega(\omega - \omega_{*i})]^{1/2}}{\omega_{A\theta}} + \beta_h \frac{1}{\varepsilon} \frac{\omega}{\omega_{dm}} \ln\left(1 - \frac{\omega_{dm}}{\omega}\right) + \delta\widehat{W}_c = 0 \quad (4)$$

Solving this equation, we can get three solutions of interest: (a) the precession fishbone with  $\omega \sim \omega_{dm}$ ; (b) the diamagnetic fishbone with  $\omega \cong \omega_{*i}$ ; (c) a damped internal kink mode.

### 3. Precession fishbone

In this section, we focus on the precession fishbone in an EAST discharge. We analyze this branch near marginal stability, giving its real frequency  $\omega_r$ , critical beta  $\beta_{h,c}$  and growth rate  $\gamma_p$  approximately. Then, numerical results are shown for this branch, indicating the behavior of  $\omega_r$  and  $\gamma_p$  as  $\beta_h$  changes.

In the limit of  $S_M \gg 1$ , i.e.  $\Lambda \gg 1$  (precession fishbone meets this condition well), equation (4) reduces to:

$$[\omega(\omega - \omega_{*i})]^{1/2} = i\omega_{A\theta} \left[ -\delta\widehat{W}_c - \beta_h \frac{\omega}{\varepsilon\omega_{dm}} \ln\left(1 - \frac{\omega_{dm}}{\omega}\right) \right] \quad (5)$$

Near marginal stability,  $\omega = \omega_{r,c} + i0^+$ , and assuming  $\omega_{*i} < \omega_{r,c} < \omega_{dm}$ , we have the real part and imaginary part of (5) separately.

$$[\omega_r(\omega_r - \omega_{*i})]^{1/2} = \pi\omega_{A\theta}\beta_{h,c} \frac{\omega_r}{\varepsilon\omega_{dm}} \quad (6)$$

$$-\delta\widehat{W}_c = \beta_{h,c} \frac{\omega_r}{\varepsilon\omega_{dm}} \ln\left(\frac{\omega_{dm}}{\omega_r} - 1\right) \quad (7)$$

So, the relation between  $\beta_{h,c}$  and  $\delta\widehat{W}_c$  reads:

$$-\delta\widehat{W}_c = \beta_{h,c} \frac{\omega_{*i}}{\varepsilon\omega_{dm}} \left[ 1 - \left( \frac{\pi\beta_{h,c}\omega_{A\theta}}{\varepsilon\omega_{dm}} \right)^2 \right]^{-1} \ln \left\{ \frac{\omega_{dm}}{\omega_{*i}} \left[ 1 - \left( \frac{\pi\beta_{h,c}\omega_{A\theta}}{\varepsilon\omega_{dm}} \right)^2 \right] - 1 \right\} \quad (8)$$

This relation divides the  $(\beta_h, \delta\widehat{W}_c)$  plane into two regions, one is stable while the other is not.

Assuming  $-\delta\widehat{W}_c \sim O(10^{-3})$ ,  $\varepsilon \sim O(10^{-2})$ , and  $\beta_{h,c} \sim O(10^{-3})$  in equation (7), we have

$$\omega_{r,c} \cong \frac{\omega_{dm}}{2} \quad (9)$$

With equation (6), we get the critical value of  $\beta_h$

$$\beta_{h,c} \cong \frac{\varepsilon\omega_{dm}}{\pi\omega_{A\theta}} \left[ 1 - \frac{2\omega_{*i}}{\omega_{dm}} \right]^{1/2} \quad (10)$$

Under the condition of  $\delta\widehat{W}_c\pi\omega_{A\theta}/\omega_{dm} \leq O(1)$ ,  $\beta_h \cong \beta_{h,c}$ , the growth rate of precession fishbone is approximated as

$$\gamma_p \cong \frac{\pi^2\omega_{A\theta}}{4\varepsilon} (\beta_h - \beta_{h,c}) \quad (11)$$

Experiment parameters from an EAST NBI discharge [6] are used here to do further study, the main parameters are:  $R_0 = 1.86m$ ,  $a = 0.44m$ ,  $n_{e0} = 5.28 \times 10^{19}m^{-3}$ ,  $r_s = 0.107m$ ,  $q_0 = 0.9150$ ,  $B_0 = 1.75T$ ,  $\beta_{total} = 0.0345$ ,  $s = \frac{r_s}{q} \frac{dq}{dr} = 0.172$ ,  $B_\theta = \frac{r_s B_0}{R_0} = 0.101T$ ,  $\rho = 1.77 \times 10^{-7}kg \cdot m^{-3}$ ,  $\omega_{A\theta} = 3.434 \times 10^5 rad/s$ ,  $\beta_p = 1.1288$ ,  $\delta\widehat{W}_c = -3.15 \times 10^{-3}$ ,  $S_M = 2 \times 10^6$ ,

$\omega_{dm} = 0.860 \times 10^5 \text{ rad/s}$ . Fixing those parameters but changing  $\beta_h$  we solve equation (4) numerically. The relation  $\omega_r$  versus  $\beta_h$  and  $\gamma_p$  versus  $\beta_h$  for precession fishbone are shown in Figure 1.

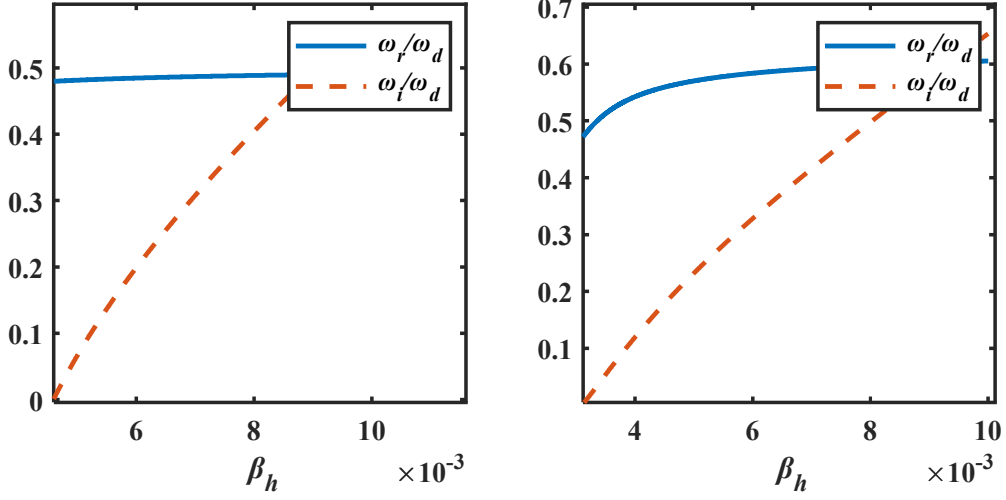


Figure 1. The real frequency (solid line) and growth rate (dotted line, both normalized by  $\omega_{dm}$ ) of precession fishbone with (a)  $\omega_{*i} = \hat{\omega}_{*e} = 0$  and (b)  $\omega_{*i} = -\hat{\omega}_{*e} = 2.2 \times 10^4 \text{ rad/s}$  versus  $\beta_h$  with real discharge parameters

This mode is excited when  $\beta_h = 0.0046$ , i.e.  $\beta_h/\beta_{total} = 0.13$ . When  $\beta_h/\beta_{total} = 0.25$ ,  $\gamma_p$  is about  $0.4620\omega_{dm} = 3.97 \times 10^4/\text{s}$ ,  $\omega_r$  is around  $0.4894\omega_{dm} = 4.21 \times 10^4/\text{s}$ . The results match well with simulation results [10].  $\omega_{*i} = 2.2 \times 10^4 \text{ rad/s}$ ,  $\hat{\omega}_{*e} = -\omega_{*i}$ ,  $\omega_{dm} = 0.860 \times 10^5 \text{ rad/s}$ , the mode is excited when  $\beta_h = 0.0031$ ,  $\omega_r$  is around  $(0.47 - 0.6)\omega_{dm}$ .

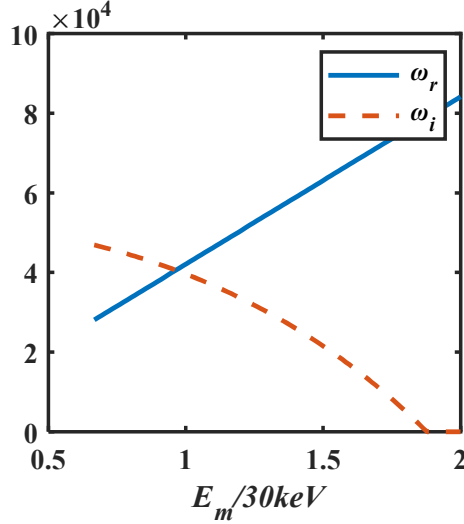


Figure 2. The real frequency (solid line) and growth rate (dotted line, both normalized by  $\omega_{dm}$ ) of precession fishbone with  $\beta_h/\beta_{total} = 0.25$  versus  $E_m$  (normalized by 30keV)

In addition, fixing  $\beta_h/\beta_{total} = 0.25$ , change the characteristic energy of deeply trapped ions from 20keV to 60keV, the result is shown in Figure 3. We find that for a certain  $\beta_h$ , growth rate decrease as precession frequency increase, while real frequency increase on the contrary.

## 4. Diamagnetic fishbone

In this section, diamagnetic fishbone in the same discharge is investigated. This branch of fishbone is one of the two  $m/n=1/1$  modes which need “viscous” from EPs to develop. We present the analytical expression of its growth rate and find this solution in numerical calculation.

Considering the ordering of  $\beta_h$ , the real part of  $\delta\widehat{W}_k$  can be neglected. We have  $\delta\widehat{W}_k = -i\pi\beta_h \frac{\omega}{\varepsilon\omega_{dm}}$ . At a limit of  $|Im(\delta\widehat{W}_k)| < -\delta\widehat{W}_c$  and  $(\omega_{A\theta}/S_M\omega_{*i})^{1/2} < -\delta\widehat{W}_c + \delta\widehat{W}_k < \omega_{*i}/\omega_{A\theta}$ , we have [11]

$$\gamma_d \cong 2\pi \frac{\beta_h}{\varepsilon} \frac{\omega_{A\theta}^2}{\omega_{dm}} (-\delta\widehat{W}_c) - \frac{5}{2} \frac{\omega_{A\theta}^3}{S_M\omega_{*i}(\omega_{*i} - \widehat{\omega}_{*e})} \quad (12)$$

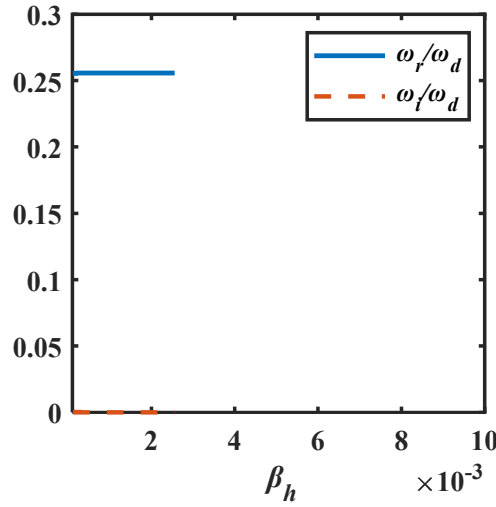


Figure 3. The real frequency (solid line) and growth rate (dotted line, both normalized by  $\omega_{dm}$ ) of diamagnetic fishbone versus  $\beta_h$  with  $\omega_{*i} = -\widehat{\omega}_{*e} = 2.2 \times 10^4 \text{ rad/s}$  and real discharge parameters

## 5. Internal kink

In this section, the lower-frequency mode is briefly discussed. This solution is recognized as a resistive internal kink mode, which is likely to be a trigger of sawtooth oscillations. It has a real frequency and growth rate

$$\omega_{rk} \cong \frac{\delta\widehat{W}_c^2 \omega_{A\theta}^2}{\omega_{*i}}$$

$$\gamma_k \cong \frac{5}{2} \frac{\omega_{A\theta}^2}{S_M\omega_{*i}\widehat{\omega}_{*e}} + 2\pi \frac{\beta_h}{\varepsilon} \frac{\delta\widehat{W}_c^3 \omega_{A\theta}^4}{\omega_{dm}\omega_{*i}}$$

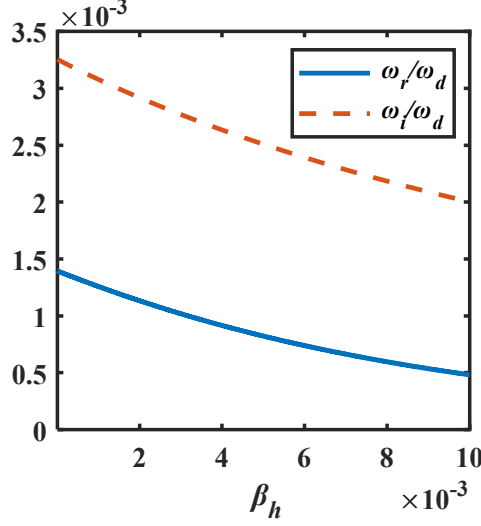


Figure 4. The real frequency (solid line) and growth rate (dotted line, both normalized by  $\omega_{dm}$ ) of internal kink versus  $\beta_h$  with  $\omega_{*i} = -\hat{\omega}_{*e} = 2.2 \times 10^4 \text{ rad/s}$  and real discharge parameters

## 6. Summary

In conclusion, detailed analysis is carried out for  $m/n=1/1$  instabilities in one EAST shot via the combined fishbone dispersion relation. Precession fishbone is found unstable when energetic ion beta exceeds a critical value, which is slightly affected by ion diamagnetic frequency. In the same discharge, according to our analysis, diamagnetic fishbone will not be excited. The real frequencies and growth rates of both solutions match the modeling results in Ref. well. These results verify the theories of *Chen* and *Coppi et al* and ensure the combined dispersion relation to become a guidance for future devices' design and operations. Besides, we propose a remaining problem that the dependence between resonance frequency and bulk plasma is not reflected well in this model. For the third interesting solution in the dispersion relation, which is called an internal kink, we calculated its frequency and growth rate. It was shown that precession fishbone has a much larger growth rate than the other two in a realistic beta range. Since the diamagnetic branch's growth rate is too low, this branch can hardly show up in this charge.

## References

- [1] K. McGuire, R. Goldston, M. Bell, M. Bitter, K. Bol, K. Brau, D. Buchenauer, T. Crowley, S. Davis, F. Dylla, H. Eubank, H. Fishman, R. Fonck, B. Grek, R. Grimm, R. Hawryluk, H. Hsuan, R. Hulse, R. Izzo, R. Kaita, S. Kaye, H. Kugel, D. Johnson, J. Manickam, D. Manos, D. Mansfield, E. Mazzucato, R. McCann, D. McCune, D. Monticello, R. Motley, D. Mueller, K. Oasa, M. Okabayashi, K. Owens, W. Park, M. Reusch, N. Sauthoff, G. Schmidt, S. Sesnic, J. Strachan, C. Surko, R. Slusher, H. Takahashi, F. Tenney, P. Thomas, H. Towner, J. Valley, and R. White, *Study of High-Beta Magnetohydrodynamic Modes and Fast-Ion Losses in PDX*, Phys.

- Rev. Lett. **50**, 891 (1983).
- [2] L. Chen, R. B. White, and M. N. Rosenbluth, *Excitation of Internal Kink Modes by Trapped Energetic Beam Ions*, Phys. Rev. Lett. **52**, 1122 (1984).
  - [3] H. Biglari and L. Chen, *Influence of Resistivity on Energetic Trapped Particle-induced Internal Kink Modes*, 6 (n.d.).
  - [4] B. Coppi and F. Porcelli, *Theoretical Model of Fishbone Oscillations in Magnetically Confined Plasmas*, Phys. Rev. Lett. **57**, 2272 (1986).
  - [5] B. Coppi, S. Migliuolo, and F. Porcelli, *Macroscopic Plasma Oscillation Bursts (Fishbones) Resulting from High-Energy Populations*, Phys. Fluids **31**, 1630 (1988).
  - [6] L. Xu, J. Zhang, K. Chen, L. Hu, E. Li, S. Lin, T. Shi, Y. Duan, and Y. Zhu, *Fishbone Activity in Experimental Advanced Superconducting Tokamak Neutral Beam Injection Plasma*, Phys. Plasmas **22**, 122510 (2015).
  - [7] G. Ara, B. Basu, and B. CoPPI, *Magnetic Reconnection and  $m = 1$  Oscillations in Current Carrying Plasmas*, 34 (n.d.).
  - [8] M. N. Bussac, R. Pellat, D. Edery, and J. L. Soule, *Internal Kink Modes in Toroidal Plasmas with Circular Cross Sections*, Phys. Rev. Lett. **35**, 1638 (1975).
  - [9] R. B. White, L. Chen, F. Romanelli, and R. Hay, *Trapped Particle Destabilization of the Internal Kink Mode*, 10 (n.d.).
  - [10] W. Shen, F. Wang, G. Y. Fu, L. Xu, G. Li, and C. Liu, *Hybrid Simulation of Fishbone Instabilities in the EAST Tokamak*, Nucl. Fusion **57**, 116035 (2017).
  - [11] R. B. White, F. Romanelli, and M. N. Bussac, *Influence of an Energetic Ion Population on Tokamak Plasma Stability*, Phys. Fluids B Plasma Phys. **2**, 745 (1990).